

Articles

Novel Extended π -Conjugated Dendritic Zn(II)-porphyrin Derivatives for Dye-sensitized Solar Cell Based on Solid Polymeric Electrolyte: Synthesis and Characterization

Min Soo Kang, Jae Buem Oh, Soo Gyun Roh, Mi-Ra Kim,[†] Jin Kook Lee,[‡] Sung-Ho Jin,^{†,*} and Hwan Kyu Kim^{*}

Center for Smart Light-Harvesting Materials and Department of Advanced Materials, Hannam University, Daejeon 306-791, Korea. *E-mail: hwankkim@hannam.ac.kr

[†]Center for Plastic Information System, Pusan National University, Busan 609-735, Korea. *E-mail: shjin@pusan.ac.kr

[‡]Department of Polymer Science and Engineering, Pusan National University, Busan 609-735, Korea

Received September 17, 2006

We have designed and synthesized three Zn(II)-porphyrin derivatives, such as Zn(II) porphyrin ([G-0]Zn-P1) and aryl ether-typed dendron substituted Zn(II)-porphyrin derivatives ([G-1]Zn-P1 and [G-1]Zn-P-CN1). Their chemical structures were characterized by ¹H-NMR, FT-IR, UV-vis absorption, EI-mass, and MALDI-TOF mass spectroscopies. Their electrochemical properties were studied by cyclic voltammetry measurement. These Zn(II)-porphyrin derivatives have been used to fabricate dye-sensitized solar cells (DSSCs) based on solid polymeric electrolytes as dye sensitizers and their device performances were evaluated by comparing with that of a standard Ru(II) complex dye. [G-1]Zn-P-CN1 showed the enhanced power conversion efficiency than those of other porphyrin derivatives, as expected. Short-circuit photocurrent density (J_{sc}), open-circuit voltage (V_{oc}), fill factor (FF), and power conversion efficiency (η) of solid-typed DSSC for [G-1]Zn-P-CN1 were evaluated to be $J_{sc} = 11.67 \text{ mA/cm}^2$, $V_{oc} = 0.51 \text{ V}$, $FF = 0.46$, and $\eta = 2.76\%$, respectively.

Key Words : Zn(II)-porphyrins, Dye-sensitized solar cell, Solid polymeric electrolyte, Power conversion efficiency

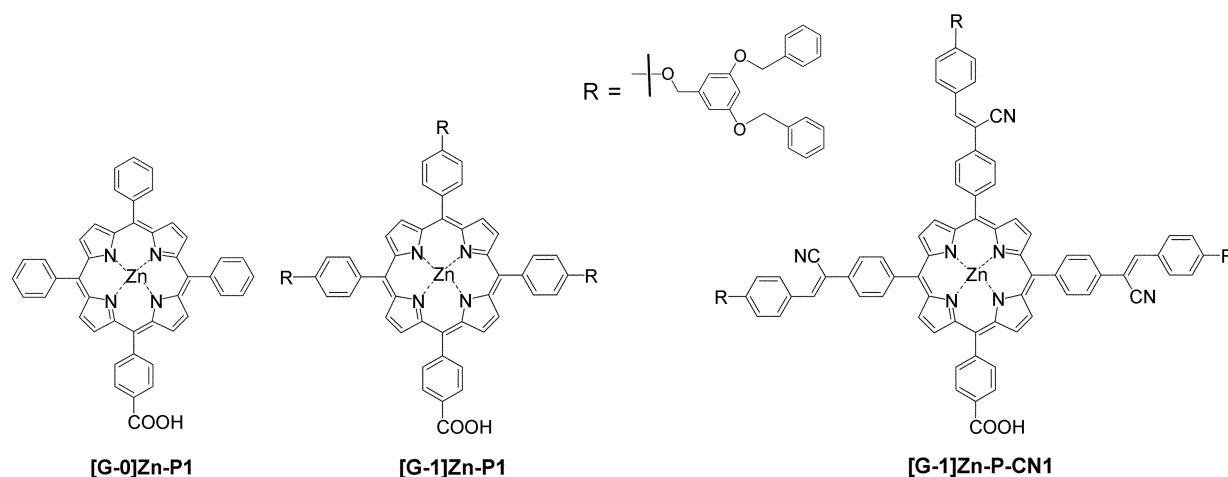
Introduction

Dye-sensitized solar cells (DSSCs) constructed using dye molecules, nanocrystalline metal oxides and organic liquid electrolytes have attracted much attention because of their high power conversion efficiency and the feasibility of the preparation. Recently, the solar power conversion efficiencies of DSSCs using ruthenium complex dyes and liquid electrolytes have reached 10.4% (100 mW/cm², AM1.5) by Grätzel group.¹ However, it has not been applied commercially yet, because of its several problems, such as the sealing to block the leakage of liquid electrolyte or expensive ruthenium complex sensitizer materials. The replacement of liquid electrolytes by solid-typed electrolytes or expensive ruthenium complex sensitizer by low cost photo-sensitizers has been ensured to solve the problems.²⁻⁴

Very recently, except for the ruthenium complexes, porphyrin species, such as the chlorophyll derivatives and Zn(II)-porphyrin complexes have been investigated as long-wavelength sensitizers on DSSCs.⁵ The use of porphyrins as light harvesters or photosensitizers on DSSCs is particularly attractive, due to their primary role in photosynthesis and the relative ease with which a variety of covalent or noncovalent porphyrin arrays can be developed. The attachment of a large porphyrin array to a nanocrystalline wide-band gap

semiconductor surface provides a way to dramatically increase the surface dye concentration and the light energy conversion efficiency of the device.

In a recent report, the power conversion efficiency was optimized for tetrakis(4-carboxyphenyl)porphyrins-based DSSCs and the addition of a coadsorbent.⁶ Very recently, Grätzel group also reported that the power conversion efficiency was improved due to the optimization of zinc metalloporphyrins-based DSSCs and the addition of a coadsorbent ($V_{oc} = 0.566 \text{ V}$, $J_{sc} = 13.5 \text{ mA/cm}^2$, and $\eta = 5.2\%$).⁷ To date, this is the best-reported value for a porphyrin photoelectrochemical cell (PEC), and was achieved using a chenodeoxycholic acid (CDCA) as a coadsorbent. In contrast, Wamser *et al.* have reported a solid state based DSSC, which uses aminophenyltricarboxy-phenylporphyrin dye (TC3APP) with an aniline gel-based electrolyte system, giving a conversion efficiency of 0.8%.⁸ The reason why porphyrin derivatives are less efficient sensitizer dyes, compared with those of ruthenium complex based dyes in DSSCs, probably arises from an increased probability of exciton annihilation. Durrant and co-workers⁹ suggested that porphyrins have a inherent tendency to aggregate, and, at high porphyrin coverage, dipole/dipole interactions are expected to allow rapid migration of the excited state between neighboring porphyrins. It leads to increase the



Scheme 1. Chemical structures of Zn(II)-porphyrin dyes.

probability of exciton annihilation. However, the low emission dipole of the metal-to-ligand charge transfer (MLCT) of a ruthenium bipyridyl complex would prevent such migration.

In this study, to reduce the probability of exciton annihilation from rapid migration of the excited state between neighboring porphyrin dyes, we report the detail of the synthesis and photo conversion efficiency of three Zn(II)-porphyrins derivatives, such as the 1st aryl ether-typed dendron substituted Zn(II)-porphyrin derivatives ([G-1]Zn-P1 and [G-1]Zn-P-CN1), and [G-0]Zn-P1 (Scheme 1). Aryl-ether typed dendron was introduced to prevent the rapid migration of the excited state between neighboring porphyrin dyes, and carboxylic acid group was selected as a binding group. To enhance the electron injection properties, cyano group was additionally incorporated into a Zn(II)-porphyrin with the stilbene moiety, yielding a [G-1]ZnP-CN1.

Experimental Section

Materials. 3,5-Dihydroxybenzoic acid, 3,5-dihydroxybenzyl alcohol, carbontetrabromide, triphenylphosphine, 4-hydroxybenzaldehyde, pyrrole, boron trifluoride diethyl-etherate (BF₃OEt₂), 2,3-dichloro-5,6-dicyano-1,4-benzoquinone (DDQ), sodium cyanide, Zn(II) acetate dihydrate and potassium tert-butoxide were purchased from Aldrich Chemical Co. and methyl-4-formylbenzoate was purchased from Fluka Co. All chemicals were used without further purification.

Characterization. The ¹H-NMR spectra were recorded at room temperature with Varian Oxford 300 spectrometers and chemical shifts were reported in ppm units with tetramethylsilane as an internal standard. FT-IR spectra were measured as KBr pellets on a Perkin Elmer Spectrometer. UV-visible absorption spectra were obtained in THF on a Perkin-Elmer Lambda 14 spectrometer or a Shimadzu UV-2401PC spectrophotometer. The corrected fluorescence emission and excitation spectra were measured on an Edinburgh FS920 fluorometer with 450 W Xe-lamp and

Hamamatsu R955 PMT. Temporal profiles of the photoluminescence (PL) decays on ns ~ ps time scale were measured by using time-correlated single photon counting method (TCSPC). Cyclic voltammetry was performed on a BAS CV-50W electrochemical analyzer with a three electrode cell, which included Ag/AgNO₃ in CH₃CN as reference electrode, carbon electrode as working electrode and Pt wire as counter electrode.

Synthesis. [G-1]-DPM, [G-1]-CHO, MEOOC-DPM and 4-bromomethylbenzaldehyde were synthesized according to previous procedures.¹⁰⁻¹⁴

[5,10,15-Triphenyl-20-(4-methoxycarbonylphenyl)porphyrin] ([G-0]FB-P): The solution of benzaldehyde (3.00 g, 28.27 mmol), pyrrole (2.53 g, 37.69 mmol) and methyl-4-formylbenzoate (1.55 g, 9.42 mmol) was condensed in CHCl₃ (942 mL) with BF₃OEt₂ (1.31 mL, 10.37 mmol) at room temperature for 1 h. Then DDQ (6.42 g, 28.27 mmol) was added, and the reaction mixture was stirred for 1 h at room temperature. The solvent was removed *in vacuo* to give a residue. The residue was then dissolved in CHCl₃ and passed through a short silica gel column to remove the non-porphyrinic components from the crude reaction mixture. After removing the solvent, the crude product was purified *via* flash column chromatography using a gradient of CHCl₃ as eluent and dried *in vacuo* to give [G-0]FB-P (0.60 g, 10%) as a purple solid. ¹H-NMR (CDCl₃, 300 MHz) [ppm]: δ 8.88-8.78 (m, 8H, β-pyrrole), 8.45-8.42 (d, 2H, *J* = 8.1 Hz, Ar-H), 8.32-8.29 (d, 2H, *J* = 8.1 Hz, Ar-H), 8.22-8.2 (d, 6H, *J* = 5.1 Hz, Ar-H), 7.80-7.83 (m, 9H, Ar-H), 4.12 (s, 3H, -OCH₃), -2.84 (s, 2H, -NH); FT-IR (KBr pellet, cm⁻¹): 1720 (ester, C=O), 3315 (amine, -NH).

[5,10,15-Triphenyl-20-(4-methoxycarbonylphenyl)porphyrin]Zinc ([G-0]Zn-P): A solution of [G-0]-FB-P (530 mg, 0.788 mmol) and zinc acetate dihydrate (865 mg, 4.00 mmol) in THF (50 mL) was refluxed for 8 hrs. The cooled reaction mixture was extracted with CH₂Cl₂ and washed with brine several times. The organic layer was dried with sodium sulfate and evaporated *in vacuo* to give [G-0]Zn-P (560 mg, 97%) as a purple solid. ¹H-NMR (CDCl₃, 300

MHz) [ppm]: δ 8.88-8.78 (m, 8H, β -pyrrole), 8.45-8.42 (d, 2H, J = 8.1 Hz, Ar-H), 8.32-8.29 (d, 2H, J = 8.1 Hz, Ar-H), 8.22-8.2 (d, 6H, J = 5.1 Hz, Ar-H), 7.80-7.83 (m, 9H, Ar-H), 4.12 (s, 3H, -OCH₃); FT-IR (KBr pellet, cm⁻¹): 1720 (ester, C=O).

5,10,15-Triphenyl-20-(4-carboxyphenyl)porphyrin[Zinc] ([G-0]Zn-P1): [G-0]ZnP (560 mg, 0.761 mmol) and KOH (427 mg, 7.600 mmol) were dissolved in THF-EtOH (1 : 1, 100 mL) and water (20 mL), and the solution was refluxed for 1 day. The reaction mixture was then cooled to room temperature and then acidified with aqueous HCl (pH \approx 2) and extracted with CH₂Cl₂. The organic phase was washed with water several times and dried with sodium sulfate. The filtrate was concentrated *in vacuo* to give [G-0]Zn-P1 (540 mg, 98%) as a purple solid. ¹H-NMR (CDCl₃, 300 MHz) [ppm]: δ 8.99-8.91 (m, 8H, β -pyrrole), 8.54-8.51 (d, 2H, J = 8.1 Hz, Ar-H), 8.38-8.35 (d, 2H, J = 8.1 Hz, Ar-H), 8.24-8.21 (d, 6H, J = 7.3 Hz, Ar-H), 7.78-7.76 (m, 9H, Ar-H); FT-IR (KBr pellet, cm⁻¹): 1690 (carboxylic acid, C=O), 2400-3400 (carboxylic acid -COOH); UV-vis (THF, nm): λ_{\max} (log ϵ) 423 (5.848), 555 (4.389), 595 (3.881); PL (THF, nm): λ_{\max} 603, 654; FAB-mass (m/e): Calcd. (720.15), Found (720).

5,10,15-Tri([G-1])₃-20-(4-methoxycarbonylphenyl)porphyrin ([G-1]FB-P): The solution of [G-1]-DPM (4.46 g, 8.25 mmol), MeOOC-DPM (2.31 g, 8.25 mmol), [G-1]-CHO (7.00 g, 16.49 mmol) was condensed in CHCl₃ (820 mL) with BF₃OEt₂ (0.7 mL, 2.47 mmol) at room temperature for 1 h. Then DDQ (5.61 g, 24.74 mmol) was added, and the reaction mixture was stirred for 1 h at room temperature. The solvent was removed under vacuum and the residue was then dissolved in CH₂Cl₂ and passed through a short silica gel column to remove the non-porphyrinic components from the crude reaction mixture. This mixture was purified with a second column (silica, CH₂Cl₂) and the organic solvent was removed *in vacuo* to give [G-1]FB-P (0.65 g, 5%) as a purple solid. ¹H-NMR (CDCl₃, 300 MHz) [ppm]: δ 8.79-8.66 (m, 8H, β -pyrrole), 8.22 (d, 2H, J = 8.1 Hz, Ar-H), 8.19 (d, 2H, J = 8.1 Hz, Ar-H), 7.98 (d, 6H, J = 8.4 Hz, Ar-H), 7.48-7.3 (m, 30H, Ar-H), 7.24 (d, 6H, J = 8.4 Hz, Ar-H), 6.84 (d, 6H, J = 2.1 Hz, Ar-H), 6.65 (t, 3H, J = 2.1 Hz, Ar-H), 5.12 (s, 6H, -CH₂), 5.08 (s, 12H, -CH₂), 4.12 (s, 3H, -OCH₃), -2.72 (s, 2H, -NH); FT-IR (KBr pellet, cm⁻¹): 1720 (ester, C=O), 3315 (amine, -NH).

[5,10,15-Tri([G-1])₃-20-(4-methoxycarbonylphenyl)porphyrin]Zinc ([G-1]Zn-P): A solution of [G-1]FB-P (250 mg, 0.15 mmol) and zinc acetate dihydrate (169 mg, 0.77 mmol) in THF was refluxed for 8 hrs. The cooled reaction mixture was extracted with CH₂Cl₂ and washed with brine several times. The organic layer was dried with anhydrous sodium sulfate and filtered off and evaporated *in vacuo* to give pure [G-1]Zn-P (250 mg, 96%) as a purple solid. ¹H-NMR (CDCl₃, 300 MHz) [ppm]: δ 8.79-8.66 (m, 8H, β -pyrrole), 8.22 (d, 2H, J = 8.1 Hz, Ar-H), 8.19 (d, 2H, J = 8.1 Hz, Ar-H), 7.98 (d, 6H, J = 8.4 Hz, Ar-H), 7.48-7.3 (m, 30H, Ar-H), 7.24 (d, 6H, J = 8.4 Hz, Ar-H), 6.84 (d, 6H, J = 2.1 Hz, Ar-H), 6.65 (t, 3H, J = 2.1 Hz, Ar-H), 5.12 (s, 6H, -CH₂),

5.08 (s, 12H, -CH₂), 4.12 (s, 3H, -OCH₃); FT-IR (KBr pellet, cm⁻¹): 1720 (ester C=O).

[5,10,15-Tri([G-1])₃-20-(4-carboxyphenyl)porphyrin]-Zinc ([G-1]Zn-P1): [G-1]ZnP (250 mg, 0.15 mmol) and KOH (83 mg, 1.50 mmol) were dissolved in THF-EtOH (1 : 1, 100 mL) and water (20 mL), and the solution was refluxed for 1 day. The reaction mixture was then cooled to room temperature and then acidified with HCl (pH \approx 2) and extracted with CH₂Cl₂. The organic phase was washed with water several times and dried with anhydrous sodium sulfate. The crude mixture was purified with a column chromatography (Silica, MC : MeOH = 1 : 2) and the solvent was removed *in vacuo* to give [G-1]Zn-P1 (220 mg, 0.13 mmol) as a purple solid. ¹H-NMR (CDCl₃, 300 MHz) [ppm]: δ 8.99-8.88 (m, 8H, β -pyrrole), 8.53-8.5 (d, 2H, J = 8.1 Hz, Ar-H), 8.36-8.34 (d, 2H, J = 8.1 Hz, Ar-H), 8.11 (d, 6H, J = 8.4 Hz, Ar-H), 7.48-7.2 (m, 36H, Ar-H), 6.84 (d, 6H, J = 2.1 Hz, Ar-H), 6.65 (t, 3H, J = 2.1 Hz, Ar-H), 5.12 (s, 6H, -CH₂), 5.08 (s, 12H, -CH₂); FT-IR (KBr pellet, cm⁻¹): 1690 (carboxylic acid, C=O), 2400-3400 (carboxylic acid, -COOH); UV-vis (THF, nm): λ_{\max} (log ϵ) 426 (5.649), 558 (4.149), 599 (3.813); PL (THF, nm): λ_{\max} 608, 658; MALDI-TOF mass (m/e): Calcd. (1674.53), Found (1676).

5,10,15-Tri(4-bromomethylphenyl)-20-(4-methoxycarbonylphenyl)porphyrin ([BrMe]FB-P): The solution of 4-bromomethylbenzaldehyde (5.00 g, 25.12 mmol), methyl-4-formylbenzoate (1.38 g, 8.37 mmol) and pyrrole (2.32 mL, 33.39 mmol) was condensed in CHCl₃ (840 mL) with BF₃OEt₂ (1.17 mL, 9.21 mmol) at room temperature for 1 h. Then, DDQ (5.70 g, 25.12 mmol) was added, and the reaction mixture was stirred for 1 h at room temperature. The solvent was removed *in vacuo*. The residue was then dissolved in CHCl₃ and purified with a column chromatography (silica, CHCl₃) and the solvent was removed *in vacuo* to give pure [BrMe]FB-P (0.60 g, 8%) as a purple solid. ¹H-NMR (CDCl₃, 300 MHz) [ppm]: δ 8.86-8.78 (m, 8H, β -pyrrole), 8.46-8.43 (d, 2H, J = 8.1 Hz, Ar-H), 8.31-8.28 (d, 2H, J = 8.4 Hz, Ar-H), 8.2-8.17 (d, 6H, J = 8.1 Hz, Ar-H), 7.80-7.78 (d, 6H, J = 8.1 Hz, Ar-H), 4.82 (s, 6H, -CH₂), 4.08 (s, 3H, -OCH₃), -2.84 (s, 2H, -NH); FT-IR (KBr pellet, cm⁻¹): 1720 (ester, C=O), 3315 (amine, -NH); UV-vis (THF, nm) λ_{\max} : 424, 555, 598; FAB-Mass (m/e): Calcd. (948.03), Found (952).

[5,10,15-Tri(4-bromomethylphenyl)-20-(4-methoxycarbonylphenyl)porphyrin]Zinc ([BrMe]Zn-P): A solution of [BrMe]FB-P (500 mg, 0.525 mmol) and zinc acetate dihydrate (577 mg, 2.630 mmol) in THF was refluxed for 8 hrs. The cooled reaction mixture was extracted with CH₂Cl₂ and washed with brine several times. The organic layer was dried with anhydrous sodium sulfate and filtered off and evaporated *in vacuo* to give pure [BrMe]Zn-P (500 mg, 93%) as a purple solid. ¹H-NMR (CDCl₃, 300 MHz) [ppm]: δ 8.96-8.88 (m, 8H, β -pyrrole), 8.42-8.39 (d, 2H, J = 8.1 Hz, Ar-H), 8.3-8.28 (d, 2H, J = 8.4 Hz, Ar-H), 8.2-8.17 (d, 6H, J = 8.1 Hz, Ar-H), 7.80-7.78 (d, 6H, J = 8.1 Hz, Ar-H), 4.86 (s, 6H, -CH₂), 4.07 (s, 3H, -OCH₃); FT-IR (KBr pellet, cm⁻¹): 1720 (ester, C=O); UV-vis (THF, nm) λ_{\max} : 424, 555,

598; FAB-Mass (m/e): Calcd. (1009.94), Found (1014).

[5,10,15-Tri(4-cyanomethylphenyl)-20-(4-methoxycarbonylphenyl)porphyrin]Zinc ([CNMe]Zn-P): A mixture of [BrMe]Zn-P (500 mg, 0.49 mmol) and sodium cyanide (121 mg, 2.46 mmol) in DMF was stirred at room temperature for 24 hrs. Then, the resulting mixture was extracted with CH₂Cl₂ and washed with brine several times. The organic layer was dried over anhydrous sodium sulfate and filtered off. A crude product was purified by column chromatography (silica, EA : MC = 1 : 20) and the solvent was removed *in vacuo* to give pure [CNMe]Zn-P (220 mg, 52%) as a purple solid. ¹H-NMR (CDCl₃, 300 MHz) [ppm]: δ 8.94-8.90 (m, 8H, β-pyrrole), 8.45-8.42 (d, 2H, *J* = 8.1 Hz, Ar-H), 8.31-8.29 (d, 2H, *J* = 8.4 Hz, Ar-H), 8.25-8.22 (d, 6H, *J* = 8.1 Hz, Ar-H), 7.74-7.72 (d, 6H, *J* = 8.1 Hz, Ar-H), 4.14 (s, 6H, -CH₂), 4.12 (s, 3H, -OCH₃); FT-IR (KBr pellet, cm⁻¹): 1720 (ester, C=O), 2250 (nitrile, -CN), 3315 (amine, -NH); UV-vis (THF, nm) λ_{max}: 424, 555, 598; FAB-Mass (m/e): Calcd. (851.2), Found (851).

[5,10,15-Tri(4-[G-1]-CN-phenyl)-20-(4-carboxyphenyl)porphyrin]Zinc ([G-1]Zn-P-CN1): A solution of [CNMe]-Zn-P (240 mg, 0.28 mmol), potassium tert-BuO⁻K⁺ (158 mg, 1.41 mmol) in distilled THF (20 mL) and tert-butanol (20 mL) was heated at 50 °C under nitrogen for 2 hrs. Then, [G-1]-aldehyde (394 mg, 0.93 mmol) was added to the reaction mixture. The reaction mixture was further heated at 50 °C for 24 hrs. The cooled reaction mixture was diluted with water and acidified with 100 mL of aqueous 1 M HCl for 1 hr. The organic layer was extracted with CH₂Cl₂ and water and dried with anhydrous sodium sulfate and filtered off. After filtration, the filtrate was evaporated and purified by short column chromatography (MC : EA = 4 : 1) to give pure [G-1]Zn-P-CN1 (300 mg, 52%) as a purple solid. ¹H-NMR (CDCl₃, 300 MHz) [ppm]: δ 9.00-8.92 (m, 8H, β-pyrrole), 8.52-8.49 (d, 2H, *J* = 7.7 Hz, Ar-H), 8.36-8.34 (d, 2H, *J* = 8.1 Hz, Ar-H), 8.30-8.27 (d, 6H, *J* = 7.7 Hz, Ar-H), 8.04-7.92 (m, 12H, Ar-H), 7.75 (s, 3H, H-C=), 7.48-7.33 (m, 30H, Ar-H), 7.06-7.03 (d, 6H, Ar-H), 6.68 (6H, S, Ar-H), 6.58 (S, 3H, Ar-H), 5.12 (s, 6H, -CH₂), 5.0-5.08 (s, 12H, -CH₂); FT-IR (KBr pellet, cm⁻¹): 1690 (carboxylic acid, C=O), 2200 (nitrile, -CN), 2400-3400 (carboxylic acid, -COOH); UV-vis (THF, nm): λ_{max} (log ε) 340 (4.8388), 430 (5.6848), 559 (4.3222), 600 (4.0414); PL (THF, nm): λ_{max} 608, 658; MALDI-TOF mass (m/e): Calcd. (2055.65), Found (2058.2).

Preparation of quasi-solid-state electrolytes. The quasi-solid-state electrolyte was composed of 24 mg of I₂, 72 mg of tetrabutylammonium iodide (TBAI), 80 mg of 1-ethyl-3-methyl imidazolium iodide as an ionic liquid, 0.32 mL of ethylene carbonate (EC)/0.08 mL of propylene carbonate (PC) (EC/PC = 4/1 as weight ratio), and a polymer matrix as polyethylene glycol (PEG, M_w = 20,000, Aldrich Co). 40 mg of the quasi-solid-state electrolyte was added into 0.4 mL of acetonitrile.

Fabrication and testing of dye-sensitized solar cells. The quasi-solid-state DSSCs were fabricated using porphyrin as a dye, TiO₂ nanoporous film with 9 nm size, and

quasi-solid-state electrolytes. *cis*-Di(thiocyanato)-*N,N'*-bis-(2,2'-bipyridyl)-4,4'-dicarboxylic acid)ruthenium(II) complex (ruthenium complex dye, Solaronix CA) was used as a dye to compared with photovoltaic performance of devices using porphyrin dye in the same condition. The DSSC was fabricated as following process:⁶ A volume of *ca.* 10 μL/cm² of the transparent pastes (Ti-Nanoxide HT, Solaronix CA) was spread on FTO glass by the doctor blade method. After heating up, the FTO glass was spread to TiO₂ nanoparticle *ca.* 100 °C for 30 min and *ca.* 450 °C for 30 min. The sintering process was completed and the TiO₂ deposited electrode was cooled down from 100 °C to *ca.* 60 °C at the controlled cooling rate of 3 °C/min to avoid cracking of the glass. Pt counter electrode was fabricated by spreading on FTO glass using the doctor blade method. After heating up, the FTO glass was spread to Pt Catalyst T/SP at 100 °C for 10 min, prior to firing at 400 °C for 30 min. The porphyrin dye was dissolved in CHCl₃ in a concentration of 20 mg per 100 mL of solution. Nanoporous TiO₂ film was dipped in this solution at room temperature for 24 hrs. Afterwards, the dye-sensitized TiO₂ electrode was rinsed with CHCl₃ and dried in air. Without a sealant, the electrolyte solution was casted onto TiO₂ electrode impregnated porphyrin dyes, and then dried at 60 °C for 2 hrs.

Photovoltaic measurements were performed using an AM 1.5 solar simulator (300 W simulator, models 81150) furnished with ARC Lamp power supply, and the intensity of the incident light was 100 mW/cm². The measurements were made on open cell and the active area was 0.25 cm². The power conversion efficiency (η) of the solar cell device was calculated by the values of open-circuit voltage (V_{oc}) and short-circuit current density (J_{sc}) using the following equation:

$$\eta = (J_{sc} * V_{oc}) * FF / P_{in}$$

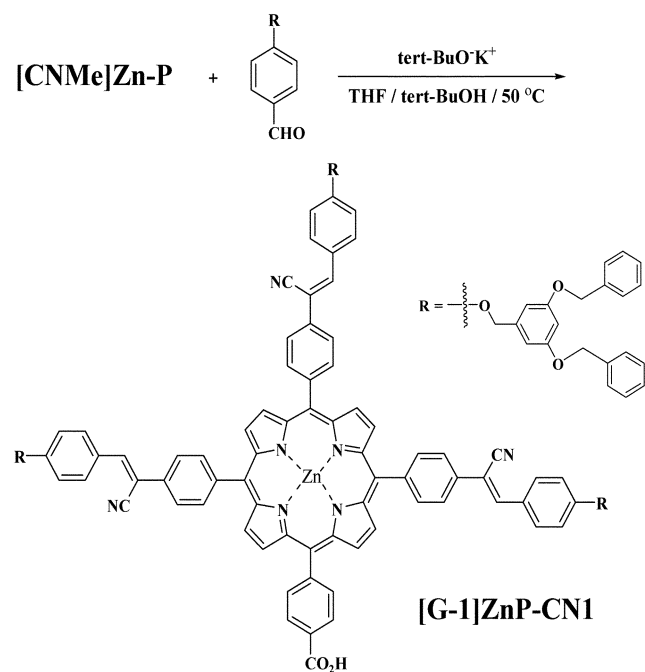
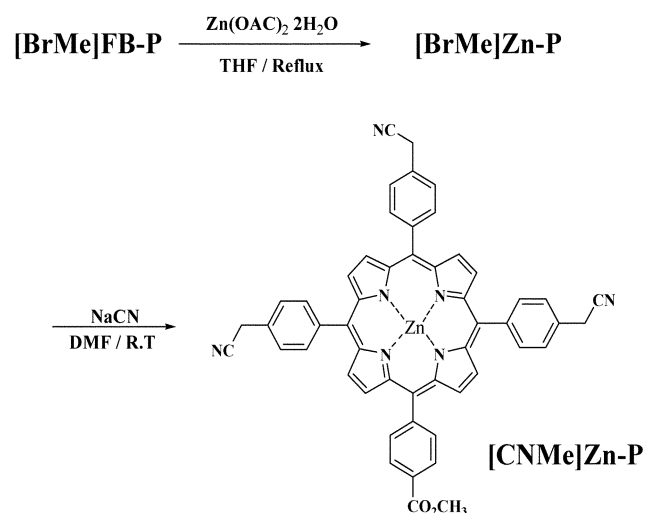
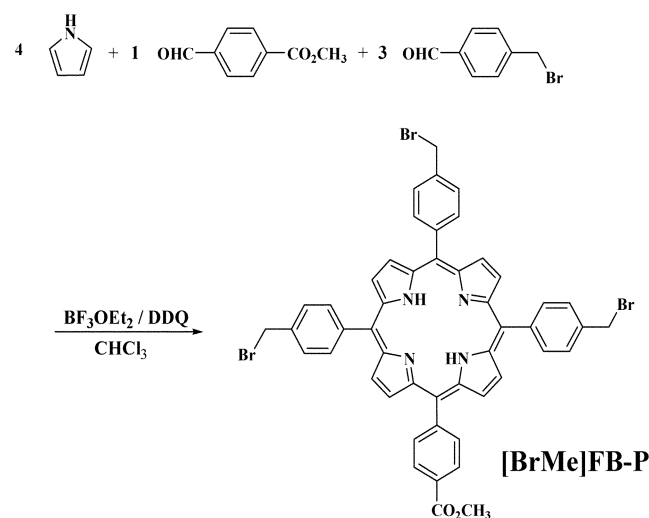
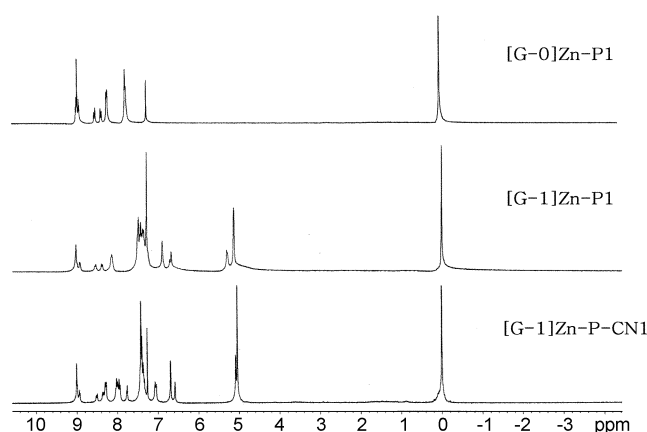
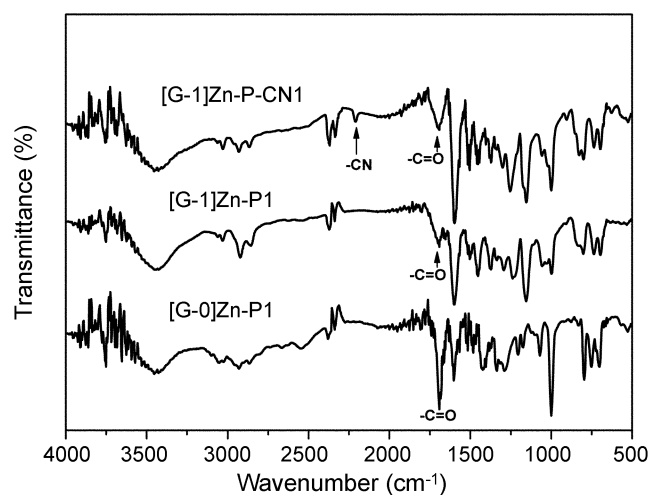
P_{in} represented the intensity of the incident light (*e.g.*, in W/m² or mW/cm²). Fill factor (FF) was calculated from the values of V_{oc} , J_{sc} , and the maximum power point, P_{max} , using the following equation

$$FF = P_{max} / (J_{sc} * V_{oc}) = (J_{max} * V_{max}) / (J_{sc} * V_{oc})$$

where J_{max} and V_{max} is maximum current density and maximum voltage, respectively.

Results and Discussion

[G-0]Zn-P1 and [G-1]Zn-P1 were prepared and identified according to the previous reports.¹⁰⁻¹⁴ The [G-1]Zn-P-CN1 was synthesized by Knoevenagel reaction between [G-1]-dendron substituted benzaldehyde and [5,10,15-tricyanomethylphenyl-20-(4-methoxycarbonylphenyl)porphyrin]zinc as a dye sensitizer (Scheme 2). The chemical structures of porphyrin derivatives were identified by ¹H-NMR, FT-IR, FAB-mass, MALDI-TOF mass, UV-vis absorption and emission spectroscopies. ¹H-NMR spectra of a free base (FB) porphyrin showed two characteristic peaks at 4.10 and -2.85 ppm, which were assigned to the methoxycarbonyl


Scheme 2. Synthetic route to [G-1]ZnP-CN1.

Figure 1. $^1\text{H-NMR}$ spectra of Zn(II)-metallo-porphyrin dyes.

Figure 2. FT-IR spectra of Zn(II)-metallo-porphyrin dyes.

group and NH group in pyrrole, respectively. NH peak of pyrrole unit was disappeared after the insertion reaction of Zn(II) dication into FB-porphyrins and the peak of methoxy group was disappeared after Knoevenagel reaction, followed by the hydrolysis of corresponding ester typed [G-1]ZnP or [G-0]ZnP. [G-1]ZnP-CN1 showed characteristic peak at 7.78 ppm which can be assigned to a vinyl group in a cyano substituted stilbene moiety (Figure 1). FT-IR spectra of porphyrin dyes commonly showed characteristic peaks at 1690 cm^{-1} , which was assigned as a carboxylic acid group. In the case of [G-1]ZnP-CN1, additional characteristic peak of cyano group was appeared at 2210 cm^{-1} (Figure 2).

In the UV-vis absorption spectra, as shown in Figure 3, each Zn(II)-porphyrin dye showed a very intense band at 430 nm for B-band, whereas the weak bands at 560 and 600 nm were assigned to the Q bands due to no d-p orbital interaction between fully occupied d orbital in Zn(II) ions and p orbital in porphyrin.¹⁵ [G-1]ZnP-CN1 showed an additional absorption band at 340 nm which corresponded to a stilbene group. Their electronic absorption, emission and electrochemical data for Zn(II)-porphyrins are summarized in Table 1. Extinction coefficient of [G-1]ZnP1 was reduced, compared with that of [G-0]ZnP1. It should result from

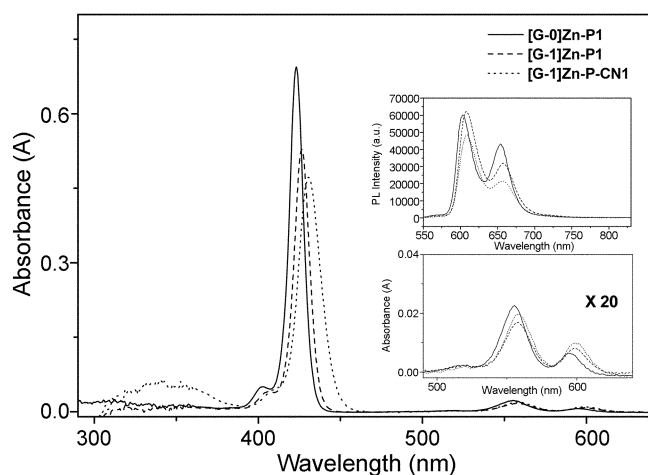


Figure 3. UV-vis absorption and emission spectra of Zn(II)-porphyrin dyes (1×10^{-6} M, THF & $\lambda_{\text{ex}} = 430$ nm).

the different chemical structure between them, since [G-1]-Zn-P1 have an electron-donating benzyloxy group in [G-0]-Zn-P1. In the case of [G-1]Zn-P-CN1, extinction coefficient of Soret absorption band was also reduced. But, Q1 band showed a similar value and Q2 band showed the increased value, as compared with that of [G-0]Zn-P1. This result indicates that cyano substituted stilbene moiety may contribute to the increased extinction coefficient value of Q2 absorption band of Zn(II)-porphyrin. With an excitation wavelength of 430 nm, their PL spectra showed two strong bands at 608 nm and a moderate band at 656 nm, which was assigned as the excited singlet state of the Zn(II)-porphyrins (Scheme 1).¹³ No emission spectra are observed for the adsorbed onto thick TiO₂ layer as a result of electron injection from the excited singlet state of the Zn(II)-porphyrins into the conduction band of the TiO₂. The time-resolved luminescence spectra in the visible region show mono-exponential decays with a luminescence lifetime of less than 2 ns for Zn(II)-porphyrins.

The electrochemical properties were investigated by cyclic voltammetry (CV) to obtain HOMO and LUMO levels of the dyes. The voltammograms were obtained from a three electrode cell in 0.1 M of *n*-Bu₄NPF₆ in CH₂Cl₂ at the scan rate of 50 mV/s, in which the electrode cell was used with Ag/AgNO₃ in CH₃CN as reference electrode, carbon electrode as working electrode and Pt wire as counter electrode (Figure 4). All the potentials are quoted vs. the ferrocene/ferrocenium (Fc/Fc⁺) couple as the internal standard. The band gap was estimated from the Q₂ edges of

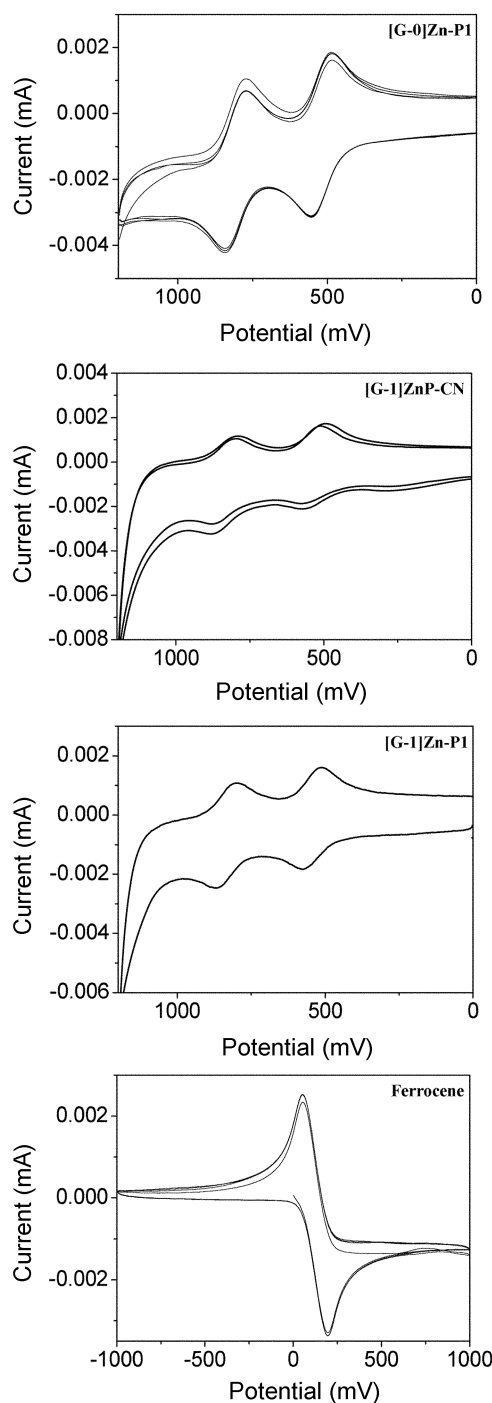


Figure 4. Cyclic voltammograms of Zn(II)-porphyrin dyes in 0.10 M tetrabutylammonium hexafluorophosphate solution in CH₂Cl₂ at scan rate of 50 mV/sec.

Table 1. The electronic absorption, emission and electrochemical data for Zn(II)-porphyrin dyes

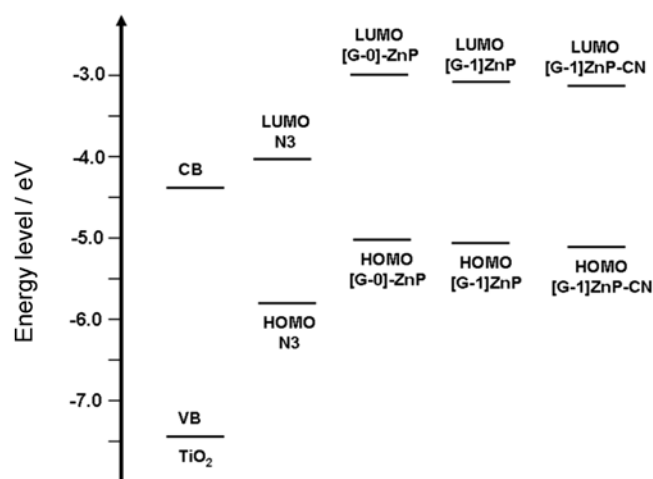
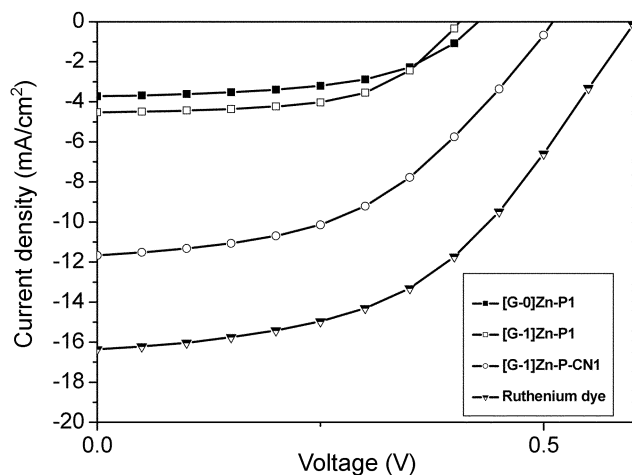
	absorption ^a λ_{max} , nm (ϵ , 10^3 M ⁻¹ cm ⁻¹)	emission ^b λ_{max} , nm	τ , ns	E _{HOMO} , ^c V	E _{LUMO} , ^d V
[G-0]Zn-P1	423 (705), 555 (24.5), 595 (7.6)	603, 654	1.9 ns	-5.10 eV	-3.07 eV
[G-1]Zn-P1	426 (446), 558 (14.1), 599 (6.5)	608, 658	1.5 ns	-5.14 eV	-3.15 eV
[G-1]Zn-P-CN1	340 (69), 430 (484), 559 (21), 600 (11)	608, 658	1.9 ns	-5.15 eV	-3.16 eV

^aUV-vis absorption data were obtained in THF solution at room temperature. ^bEmission spectra were obtained at room temperature in THF by exciting at 430 nm. ^cElectrochemical measurements were performed at room temperature using cyclic voltammetry on solution in CH₂Cl₂ containing 0.1 M *n*-Bu₄NPF₆ as the supporting electrolyte. Potentials are quoted to ferrocene (Fc/Fc⁺). ^dLUMO level was derived from HOMO energy level and the band gap.

Table 2. Performance characteristic of the DSSC devices using Zn(II)-porphyrin or ruthenium complex as sensitizers

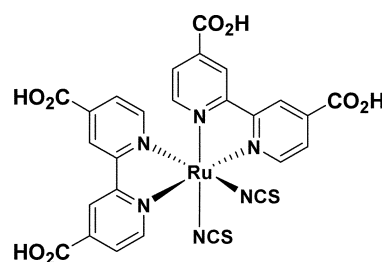
	V_{oc} (V)	J_{sc} (mA/cm ²)	Fill Factor	Efficiency (%)
[G-0]Zn-P1	0.43	3.73	0.54	0.87
[G-1]Zn-P1	0.41	4.53	0.58	1.07
[G-1]Zn-P-CN1	0.51	11.67	0.46	2.76
N3 dye	0.6	16.36	0.48	4.69

^aThe illumination is 100 mW/cm² under AM 1.5. The electrolyte is quasi-solid-state polymeric electrolyte.

**Figure 5.** Overview of the evaluated energy levels of Zn(II)-porphyrin dyes (CB: conduction band; VB: valance band).**Figure 6.** I-V curves of the DSSC devices using Zn(II)-porphyrin dyes or ruthenium complex as sensitizers under AM 1.5, 100 mW/cm².

UV-vis spectra. From the oxidation potential, HOMO energy level was derived by assuming that the energy level of Fc/Fc⁺ is 4.8 eV. Finally, their LUMO energy level was derived from HOMO energy level and the band gap (see Table 1).

The DSSC based on solid polymeric electrolyte was fabricated according to the previous report.¹⁶ The photovoltaic properties of the DSSCs using Zn(II)-porphyrin derivatives or ruthenium complex for comparison were

**Scheme 3.** Chemical structure of N3 dye.

measured under AM1.5. The performance characteristics of the DSSCs are summarized in Table 2. Figure 6 shows the current density-voltage curves obtained for the DSSCs in illumination under AM1.5 condition. The present Zn(II)-porphyrin derivatives have an appropriate LUMO level that resides above the conduction band of the TiO₂ and a HOMO level that lies below the redox potential. The relative LUMO and HOMO energy levels estimated by using cyclic voltammetry are listed in Table 1. The LUMO levels of [G-0]ZnP1, [G-1]ZnP1, and [G-1]ZnP-CN1 (Figure 5) as -3.07, -3.15, and -3.16 eV (SCE) were higher than the conduction band of TiO₂, just as that of N3 dye (Scheme 3). [G-1]ZnP-CN1, which has lower LUMO level, showed the highest value of short-circuit photocurrent density compared with those of other porphyrin derivatives such as [G-0]ZnP1 and [G-1]ZnP1. Short-circuit photocurrent density (J_{sc}), open-circuit voltage (V_{oc}), fill factor (FF), power conversion efficiency (η) of DSSC for [G-0]ZnP1 and [G-1]ZnP1 were $J_{sc} = 3.73$ mA/cm² and 4.53 mA/cm², $V_{oc} = 0.43$ V and 0.41 V, FF = 0.54 and 0.58, $\eta = 0.87$ and 1.08% respectively. In contrast to these porphyrin dyes, [G-1]ZnP-CN1 dye showed rapidly enhanced value $J_{sc} = 11.67$ mA/cm², $V_{oc} = 0.51$ V, FF = 0.46, and $\eta = 2.76\%$. In the same conditions, photovoltaic properties for ruthenium complex dye was $J_{sc} = 16.36$ mA/cm², $V_{oc} = 0.60$ V, FF = 0.48, and $\eta = 4.69\%$.

Conclusions

We have successfully designed and synthesized novel 1st aryl ether-typed dendron substituted Zn(II)-porphyrin derivatives with a cyano substituted stilbene moiety in the meso position for DSSC devices as a long-wavelength dye sensitizer. [G-0]ZnP-based device showed power conversion efficiency of $\eta = 0.8\%$ in the solid state electrolyte which is well agreed with the result of Wamser *et al.*⁸ [G-1]ZnP1 improved the power conversion efficiency ($\eta = 1.07\%$) a little bit. [G-1]ZnP-CN1 showed the significantly increased power conversion efficiency compared with those of other porphyrin dyes due to efficient electron injection by introducing cyano groups as expected ($\eta = 2.76\%$). This is an encouraging result for a porphyrin dye and it offers potential for porphyrins as alternatives to ruthenium-based dyes in the DSSC.

Acknowledgments. This research work was financially supported from the Korea Ministry of Science and Techno-

logy through National Research Laboratory Program at Hannam University and Busan National University.

References

1. Nazeeruddin, M. K.; Pechy, P.; Renouard, T.; Zakeeruddin, S. M.; Humphry-Baker, R.; Comte, P.; Liska, P.; Cevey, L.; Costa, E.; Shklover, V.; Spiccia, L.; Deacon, G. B.; Bignozzi, C. A.; Grätzel, M. *J. Am. Chem. Soc.* **2001**, *123*, 1613.
 2. Cao, F.; Oskam, G.; Searson, P. C. *J. Phys. Chem.* **1995**, *99*, 17071.
 3. Matsumoto, M.; Miyazaki, H.; Matsuihiro, K.; Kumashiro, Y.; Takaoka, Y. *Solid State Ionics* **1996**, *89*, 263.
 4. Kubo, W.; Kitamura, T.; Hanabusa, K.; Wada, Y.; Yanagida, S. *Chem. Commun.* **2002**, *4*, 374.
 5. Kay, A.; Humphry-Baker, R.; Grätzel, M. *J. Phys. Chem.* **1994**, *98*, 952.
 6. Cherian, S.; Wamser, C. C. *J. Phys. Chem. B* **2000**, *104*, 3624.
 7. Wang, Q.; Campbell, M. W.; Bonfantani, E. E.; Jolley, K. W.; Officer, D. L.; Walsh, P. J.; Gordon, K.; Humphry-Baker, R.; Nazeeruddin, M. K.; Grätzel, M. *J. Phys. Chem. B* **2005**, *109*, 15397.
 8. (a) Wamser, C. C.; Kim, H. S.; Lee, J. K. *Opt. Mat.* **2002**, *21*, 221. (b) Campbell, W. M.; Burrell, A. K.; Officer, D. L.; Jolley, K. W. *Coord. Chem. Rev.* **2004**, *248*, 1363.
 9. Tachibana, Y.; Haque, S. A.; Mercer, I. P.; Durrant, J. R.; Klug, D. R. *J. Phys. Chem. B* **2000**, *104*, 1198.
 10. Hawker, C. J.; Frechet, J. M. J. *J. Am. Chem. Soc.* **1990**, *112*, 7638.
 11. Lee, C. S.; Lindsey, J. S. *Tetrahedron* **1994**, *50*, 133.
 12. Ka, J.-W.; Kim, H. K. *Tetrahedron Lett.* **2004**, *45*, 4519.
 13. Oh, J. B.; Nah, M. K.; Kim, Y. H.; Kim, H. K. *J. Lumin.* **2005**, *111*, 255.
 14. Oh, J. B.; Nah, M. K.; Kim, Y. H.; Kang, M. S.; Kim, H. K. *Adv. Funct. Mater.* in press (2007).
 15. Oh, J. B.; Paik, K. L.; Ka, J. W.; Roh, S. G.; Nah, M. K.; Kim, H. K. *Mater. Sci. Eng. C* **2004**, *24*, 257.
-